Marine and Petroleum Geology 164 (2024) 106824

Contents lists available at ScienceDirect

Marine and Petroleum Geology

journal homepage: www.elsevier.com/locate/marpetgeo

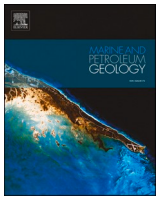

Evaluation of shale oil and gas plays - Part I: Shale reservoir property modelling of the North Sea Kimmeridge Clay Formation

Akinniyi A. Akinwumiju *, Dorothy Satterfield, Jordan J.J. Phethean

School of Built and Natural Environment, College of Science and Engineering, University of Derby, DE22 1GB, UK

ARTICLE INFO

Keywords:
Kimmeridge Clay Formation
UK North Sea
Unconventional resources
Shale reservoir properties
Artificial neural networks
3D geostatistical modelling
Sweet spots

ABSTRACT

The Kimmeridge Clay Formation (KCF) forms the source rock for most conventional hydrocarbon accumulations within the UK North Sea. However, only a few previous studies have analyzed the potential of the KCF for unconventional resources (i.e., shale oil and gas).

Here, we use machine learning techniques combined with established rock property equations to generate geochemical, petrophysical and geomechanical logs for 16 wells within Quadrant 15 of the Outer Moray Firth, UK North Sea. The neural network models used to generate geochemical logs are trained using the Levenberg-Marquardt backpropagation algorithm. The generated well logs and new KCF depth maps, constrained by an existing Base Cretaceous Unconformity (BCU) map of the UK North Sea and well top information from 48 wells, are used for 3D geostatistical modelling of KCF properties across the area. The resulting KCF property maps allow us to assess the shale oil and gas play potential across the region.

Our results suggest good organic richness and hydrocarbon yield potential for the KCF within the study area, with up to 9 wt% original total organic carbon (TOC_o), 48 mg/g original hydrocarbon yield (S_{2o}), and 607 mg/gTOC original hydrogen index (HI_o). Modelled total porosity values range between 2 and 13%, and brittleness indices lie between 25 and 65%, within the range reported for proven shale oil and gas plays.

A sweet spot map, created by integrating our modelled KCF properties, indicates prospective areas for shale oil and gas exploitation within the central Witch Ground Graben, and to a lesser extent areas of the Piper Shelf and Claymore-Tartan Ridge. These areas show good potential based on all investigated properties, with respect to industry standards.

1. Introduction

Assessment of the potential for residual shale oil and gas exploitation from geological formations can be conducted by 3D geostatistical modelling of the distribution of key geochemical, petrophysical and geomechanical properties (Johnson et al., 2018; Alshakhs and Rezaee, 2019). Traditionally, geostatistical property modelling allows estimation of the distribution of properties between available wells, while preserving the realistic reservoir heterogeneity present in well data (Schlumberger, 2019). This modelling process requires continuous values (logs) for the properties to be investigated.

Hydrocarbon source rocks are characterised by high amount of Type I or Type II organic matter that is normally investigated using total organic carbon (TOC), hydrocarbon yield (S_2) and hydrogen index (HI) parameters (Cornford, 1998; Johnson et al., 2018). However, in addition to the organic matter content, successful shale oil and gas plays have good hydrocarbon retention and hydraulic fracturing capabilities based on their porosities and brittleness (Jarvie, 2012a, 2012b; Hu et al., 2021). These key parameters have been utilized in the evaluation of the Kimmeridge Clay Formation (KCF) potential for shale oil and gas plays in this study.

Recently, various machine learning techniques including fuzzy systems, functional neural networks, and support vector machines have been employed by several authors (Kadkhodaie-Ilkhchi et al., 2009; Mahmoud et al., 2017; Yu et al., 2017; Johnson et al., 2018) to estimate continuous values for total organic carbon and other geochemical parameters of hydrocarbon source rocks based on wireline log responses (e.g. gamma ray, density, neutron, resistivity and acoustic). However, continuous values for petrophysical and geomechanical properties are normally estimated using established property equations (e.g. Jin et al., 2014; Labani and Rezaee, 2015; Alshakhs and Rezaee, 2019).

The KCF is the main source rock for the numerous conventional oil

* Corresponding author.
E-mail address: a.akinwumiju2@unimail.derby.ac.uk (A.A. Akinwumiju).

https://doi.org/10.1016/j.marpetgeo.2024.106824
Received 7 June 2023; Received in revised form 22 March 2024; Accepted 24 March 2024
Available online 27 March 2024

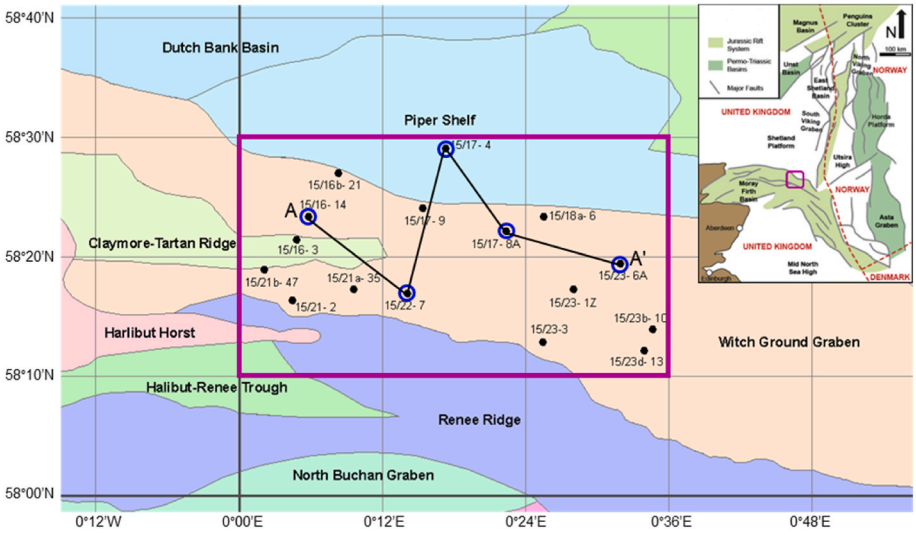

Fig. 1. Structural element map of the study area (purple box) showing selected wells for modelling inputs. The study area encompasses Blocks 16–18 and 21–23 in Quadrant 15, Outer Moray Firth region of the UK North Sea (inset modified after Raji et al., 2015). The well correlation A-A' (Fig. 11) is indicated by blue circles and black line.

Table 1
Evaluation criteria for unconventional resource plays.

Reservoir property	Industry threshold	Comments
TOC_o (wt%)	>2	>5 wt% indicates very rich shales
S_{2o} (mg/g)	10–20	>20 mg/g suggests excellent hydrocarbon yield
HI_o (mg/gTOC)	>250	Typically between 250 and 800 mg/gTOC
TP (%)	3–15	Typically between 4 and 7%
BI (%)	>32	>48% suggests high frackability

and gas discoveries in the UK North Sea Basin (Cornford, 1998) and may present a substantial unconventional resource for the UK particularly during the transition to net-zero energy. Whilst onshore production of shale oil and gas has not materialised in the UK and alternative forms of energy are increasing, the exploration of shale oil and gas in the UK North Sea could reduce environmental and safety concerns, while existing infrastructure (i.e., platforms and pipelines) could also help in the economics of offshore production (Cornford et al., 2014).

This study therefore utilises 3D geostatistical modelling of the distribution of key geochemical, petrophysical and geomechanical properties for the KCF from 16 drilled well locations to investigate the potential of shale oil and gas plays within Quadrant 15 in the Outer Moray Firth region of the UK North Sea. These wells have been selected based on the availability of appropriate wireline log data for estimating continuous data for the investigated reservoir properties. Geochemical properties include original total organic carbon (TOC_o), hydrocarbon yield (S_{2o}) & hydrogen index (HI_o), while total porosity (TP) and the brittleness index (BI) form our petrophysical and geomechanical properties, respectively.

The study area covers six blocks (blocks 16–18 and 21–23) within Quadrant 15 in the Outer Moray Firth region of the UK North Sea (Fig. 1) with an area extent of 1200 km^2. The KCF is well-developed in the study area and consists of predominantly shale lithologies with reported thicknesses of up to 600 m in wells within the Witch Ground Graben.

In general, geostatistical property modelling processes directly allow for the realistic integration of shale reservoir properties and identification of prospective area(s) for shale oil and gas plays (i.e., sweet spots), particularly after application of the industry standard thresholds for unconventional resources shown in Table 1 (Wang and Gale, 2009; Jarvie, 2012a; Perez and Marfurt, 2013; Andrews, 2014; Jiang et al., 2016; Alshakhs and Rezaee, 2019). It is worth noting that there are other economic criteria that need to be evaluated, including hydrocarbon saturation and in-place volumes. However, the richness of the data allows for a case study that develops a technique for application in more economically prospective areas.

2. Geological setting

The North Sea Basin is a proven oil and gas basin that developed as a triple junction rift system between the Moray Firth, Viking Graben, and Central Graben basins (Erratt et al., 1999; Mackay et al., 2005; Underhill and Richardson, 2022). The development of the North Sea basin has been mostly attributed to Permo-Triassic and Late Jurassic-Early Cretaceous rifting events, including accompanying episodes of thermal subsidence (Fig. 2).

The main structural elements of the North Sea Basin were developed during the Late Jurassic to Early Cretaceous extensional phase, which strongly influenced the deposition of Jurassic sediments, together with locally occurring rift associated halokinesis (Johnson et al., 2005). The highly organic-rich KCF was deposited during this extensional phase under restricted marine conditions in water depths of about 150 to more than 200 m (Fraser et al., 2002; Gallois, 2004).

The KCF consists of dark-grey brown to black shales, of calcareous to non-calcareous nature, interbedded with thin siltstone and sandstone layers (Fig. 2). It has a maximum depositional thickness of ~1400 m in depocenters within the Central and Northern North Sea regions (British Geological Survey, 2022). Within the study area, the KCF is composed of predominantly shale lithology, and is found across the basin with reported thicknesses between 20 and 600 m (Oil and Gas Authority, UK, 2019).

Further details of the geological evolution of the North Sea Basin are discussed widely elsewhere, and the reader is referred to the wider literature (e.g. Evans et al., 2003; Glennie, 1998; Johnson et al., 2005; Erratt et al., 2010; Raji et al., 2015; Underhill and Richardson, 2022).

3. Modelling inputs and processes

3D geostatistical modelling of the distribution of reservoir properties for the KCF has been conducted with Petrel reservoir modelling software. The main inputs are top and base KCF depth structure maps, for defining model boundaries, and estimated well logs of investigated properties from 16 wells. The key steps involved in building the property

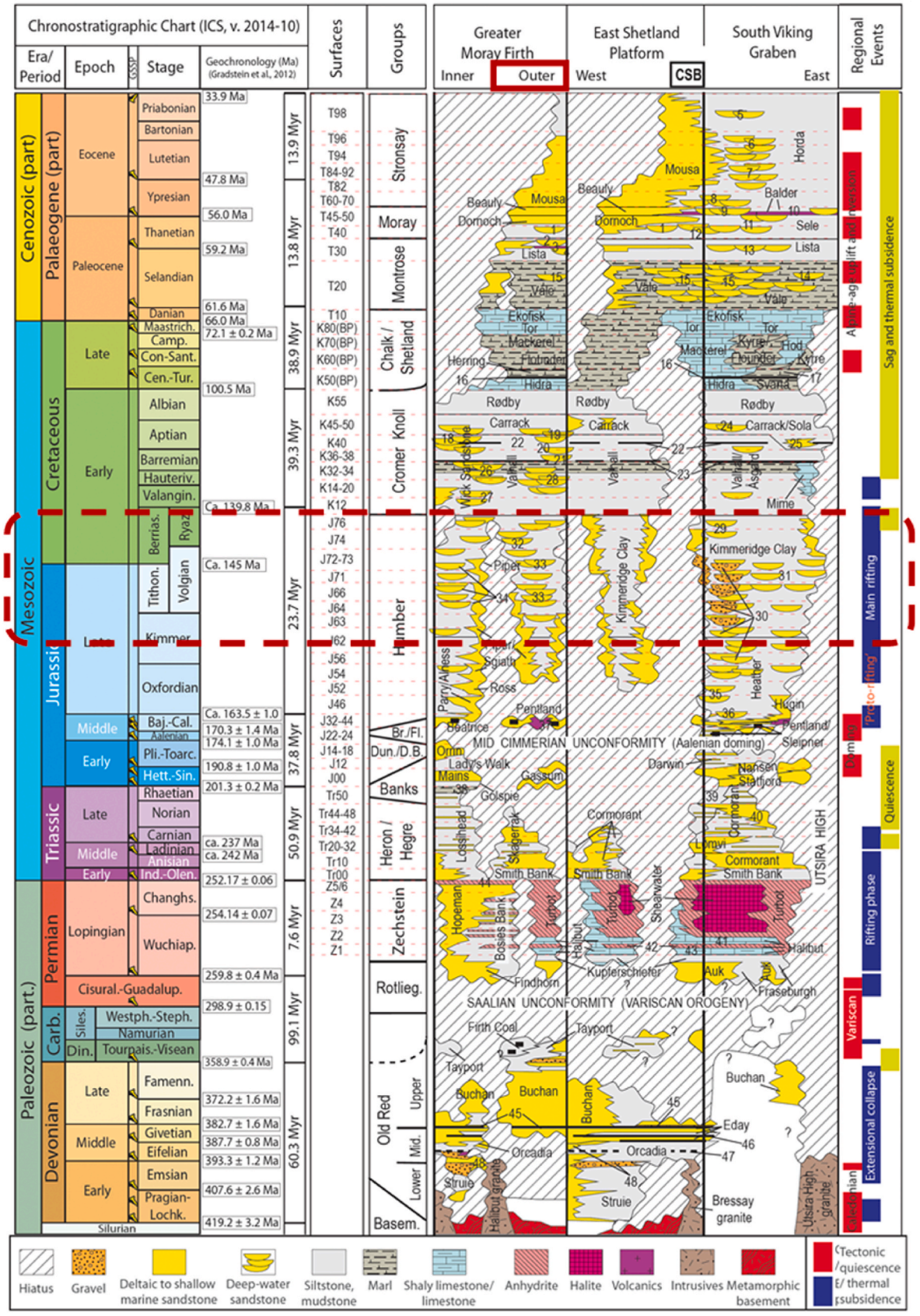

Fig. 2. Tectono-stratigraphic chart showing the regional events and KCF (dark red dashed box) in the UK North Sea (modified from Patruno and Reid, 2016).

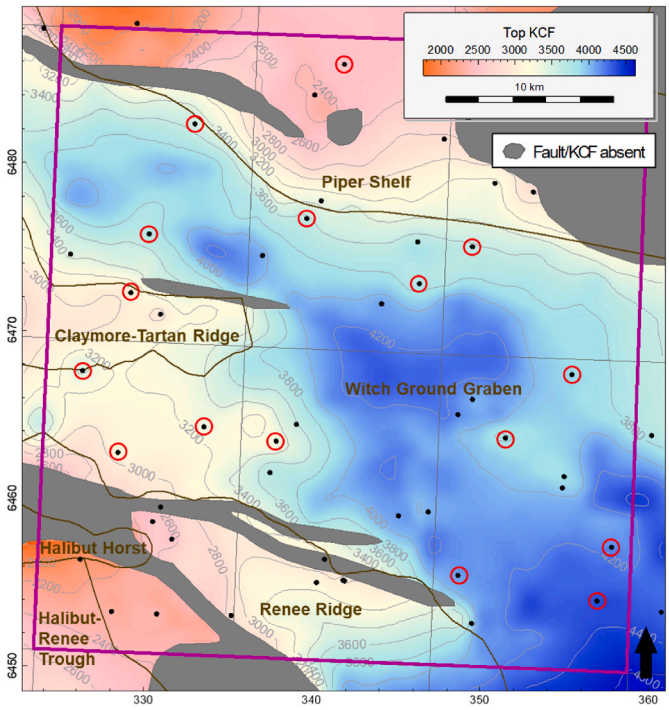

Fig. 3. Top KCF structural depth map. This map has been created using well top information from wells that penetrated the KCF interval in the study area. Wells used for training the machine learning algorithms/predicting rock properties are indicated in red circles.

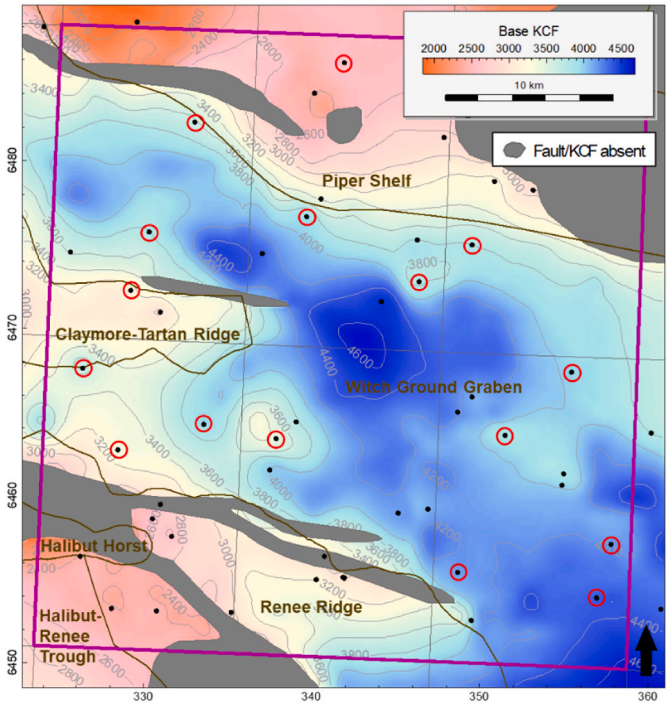

Fig. 4. Base KCF structural depth map. This map has been created using thickness information from wells that penetrated the KCF interval in the study area. Wells used for training the machine learning algorithms/predicting rock properties are indicated in red circles.

models are well correlation, structural modelling and petrophysical modelling.

3.1. Modelling inputs

3.1.1. KCF depth structure maps

The top and base KCF depth structure maps used in this modelling study were created using well top information from 48 wells within the study area and grid- and isopach-creation tools in ZetaWare's Trinity software. For the top KCF map (Fig. 3.), available well top data was interpolated geologically by correlation gridding with an existing Base Cretaceous Unconformity (BCU) map of the UK North Sea. The well top data and BCU map were obtained from the Oil and Gas Authority data repository that was published in 2019. The top KCF depth map and thickness information created from 48 wells that penetrated the KCF interval in the study area were then used to generate a base KCF depth map (Fig. 4).

3.1.2. Geochemical property logs

Trained neural network models have been created to predict continuous total organic carbon (TOC), remaining hydrocarbon yield (S_2) and hydrogen index (HI) values for the KCF in 16 well locations within the study area (Figs. 3–4) using the Neural Net Fitting application in MATLAB. Neural networks are one of the regression methods within supervised machine learning where a model can be trained to predict future output based on previous known numeric input and output data (MathWorks, 2020). Neural networks provide a variety of benefits, including ability to satisfactorily model highly nonlinear systems and recognise all possible interactions between input and output variables, accessibility to various training algorithms and the ability for trained models to be constantly updated with new data ((Tu, 1996) Kadkhodaie-Ilkhchi et al., 2009; MathWorks, 2020).

This process has used wireline logs and measured geochemical data as the training inputs and outputs respectively. Inputs are related to the desired outputs by a number of interconnected neurons, and the network is trained by iteratively modifying the strength of the connections to correctly map the given input to output response.

The training algorithm for the networks is the Levenberg-Marquardt backpropagation algorithm, which requires less training time compared to other algorithms (e.g. Bayesian Regularization, or Scaled Conjugate Gradient (MathWorks, 2020)). The performance of the networks have been evaluated using the regression R value, which measures the correlation between actual and target outputs.

3.1.2.1. Network training data. The training of the networks was conducted using a large set of KCF geochemical data (225 data points) from the analysis of core plugs from 64 wells in the larger Central North Sea region of the UK with known depth locations, allowing for determination of the corresponding wireline log value with low uncertainty compared to drill cuttings (Johnson et al., 2018). Examples of measured geochemical data and their corresponding wireline log values used in training neural network models in four wells locations are indicated in Table 2. Geochemical parameters normally relate to wireline log data (Fig. 5), where, in theory, the stronger the relationship between geochemical parameters and wireline logs, the more accurate the predictions (Kadkhodaie-Ilkhchi et al., 2009; Johnson et al., 2018; Alshakhs and Rezaee, 2019).

3.1.2.2. Network training process. Three neural network models have been trained for predicting continuous TOC, S_2 and HI data with each network having 10 hidden layer neurons (Fig. 6). For the training, the available wireline log and measured geochemical data were randomly divided into three sets in MATLAB, with 70% of the data used for training the network, 15% used for validation in order to minimise overfitting and the remaining 15% of the data used to ascertain the accuracy of the network.

Table 2
Geochemical and wireline log data used in model training in four well locations.

Well	Location	Depth (m)	TOC (wt%)	S_2 (mg/g)	HI (mg/gTOC)	T-max (°C)	Density (g/cm^3)	Neutron (v/v)	Acoustic (μs/ft)	Gamma (gAPI)
12/23- 2	Inner Moray Firth Basin	950.37	10.80	22.12	205	423	2.01	0.45	126.67	90.39
12/23- 2	Inner Moray Firth Basin	1149.10	5.70	22.20	389	429	2.28	0.37	115.38	112.56
12/23- 2	Inner Moray Firth Basin	1250.14	6.70	17.69	264	417	2.26	0.38	111.00	119.13
12/23- 2	Inner Moray Firth Basin	1340.82	7.70	29.87	388	422	2.27	0.39	111.00	132.00
12/23- 2	Inner Moray Firth Basin	1378.46	6.40	11.82	185	410	2.24	0.39	103.56	203.88
13/27- 1A	Inner Moray Firth Basin	1763.27	10.00	42.00	420	430	2.39	0.38	86.72	107.11
13/27- 1A	Inner Moray Firth Basin	1805.33	5.90	18.60	315	429	2.47	0.16	96.81	60.02
13/27- 1A	Inner Moray Firth Basin	1822.70	9.10	42.30	465	434	2.32	0.34	98.96	114.26
13/27- 1A	Inner Moray Firth Basin	1838.55	7.00	26.00	371	427	2.30	0.33	103.53	87.37
13/27- 1A	Inner Moray Firth Basin	1887.93	6.80	22.70	334	427	2.41	0.27	91.42	83.57
13/27- 1A	Inner Moray Firth Basin	1943.10	4.80	20.70	431	428	2.43	0.26	93.62	99.86
13/27- 1A	Inner Moray Firth Basin	2025.09	6.10	27.00	443	427	2.34	0.38	101.26	152.61
13/27- 1A	Inner Moray Firth Basin	2048.26	7.70	27.60	358	429	2.34	0.40	107.81	168.94
13/27- 1A	Inner Moray Firth Basin	2060.45	7.90	32.10	406	426	2.39	0.40	105.83	158.32
13/27- 1A	Inner Moray Firth Basin	2065.02	7.80	18.00	231	416	2.38	0.41	107.48	164.46
14/19- 3	Witch Ground Graben	2347.57	7.10	36.30	511	418	2.21	0.45	115.94	86.66
14/19- 3	Witch Ground Graben	2363.11	6.70	34.40	513	422	2.34	0.38	106.98	93.69
15/24a- 2	Witch Ground Graben	3784.40	1.60	2.01	126	441	2.42	0.29	99.73	156.24
15/24a- 2	Witch Ground Graben	3787.14	6.00	10.79	180	450	2.44	0.31	99.67	151.86
15/24a- 2	Witch Ground Graben	3789.88	2.40	3.78	158	445	2.54	0.20	80.78	97.52
15/24a- 2	Witch Ground Graben	3802.68	2.40	2.65	110	443	2.52	0.20	79.61	91.85
15/24a- 2	Witch Ground Graben	3811.83	2.70	4.15	154	450	2.57	0.19	80.05	103.94
15/24a- 2	Witch Ground Graben	3816.71	3.10	5.63	182	447	2.58	0.21	82.60	95.67
15/24a- 2	Witch Ground Graben	3822.80	1.00	0.73	73	450	2.63	0.13	71.71	67.81

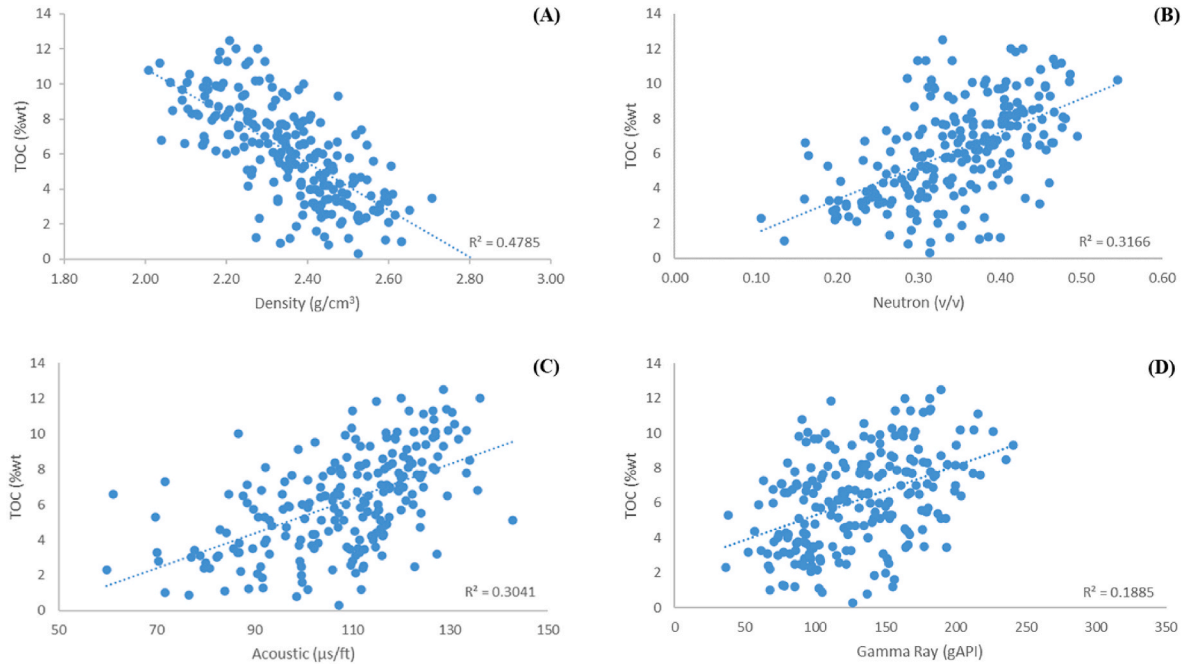

Fig. 5. Cross plots showing relationship between measured TOC and density (A), neutron (B), acoustic (C), and gamma ray (D) from core plugs, UK Central North Sea.

Several training iterations were performed to achieve optimum trained networks while observing the regression R values, which measure the correlation between outputs and targets for training, validation and test data sets. Overall, the optimum trained networks produced good quality regression lines with R values mostly greater than 0.80 for training, validation and test iterations (Figs. 7–9). The optimum target and output of R obtained for the trained networks fall within the range reported in published literature (e.g. Kadkhodaie-Ilkhchi et al., 2009; Khoshnoodkia et al., 2011; Johnson et al., 2018). Therefore, the model precision is considered to be satisfactory. However, it is noted that the model could be updated to further improve this precision once more training data is available in the future.

The trained neural network models were then used to estimate continuous TOC, S_2 and HI data (logs) for the KCF in 16 wells selected for modelling in this study. The estimated datasets show good correlations with the available laboratory measured geochemical values from the analysis of KCF samples in the studied wells (Fig. 10), and were subsequently corrected for maturity and restored to their original values (TOC_o, S_{2o} & HI_o) prior to modelling.

3.1.3. *Petrophysical and geomechanical property logs*

Alongside the geochemical properties determined above,

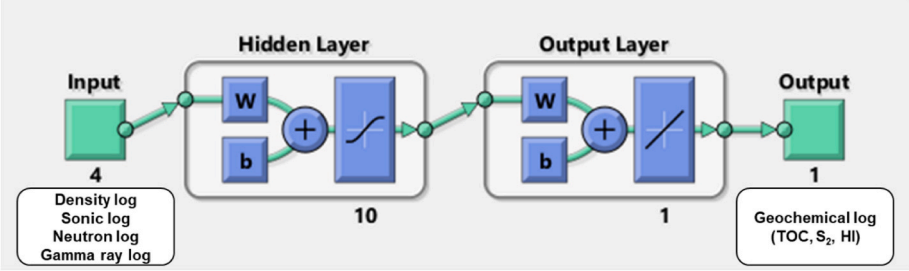

Fig. 6. Schematic of the trained neural network in MATLAB. W represents weight; b represents bias (MathWorks, 2020).

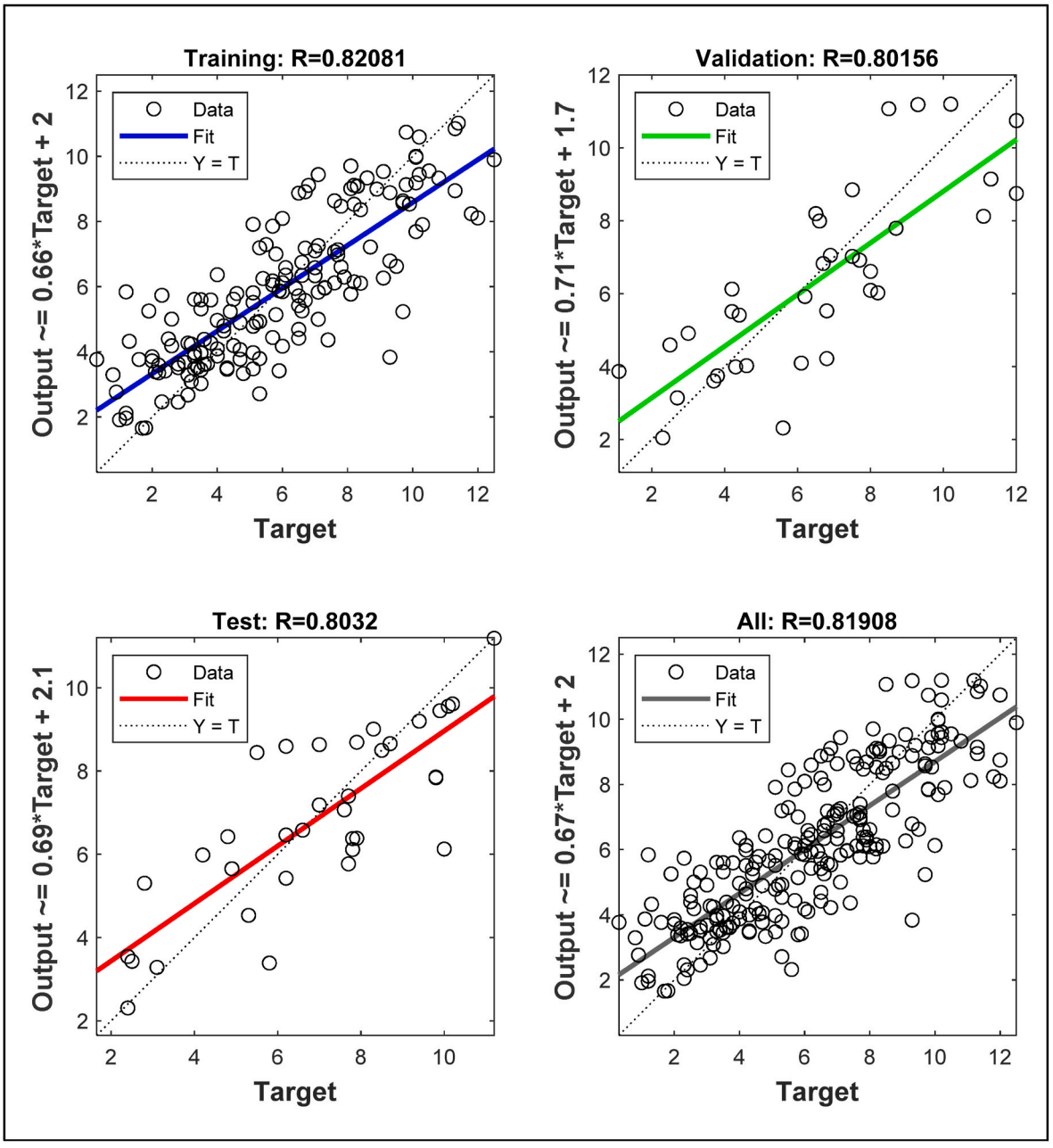

Fig. 7. Regression plots showing the correlation coefficients between target and predicted TOC values (wt%) for training, validation and test iterations.

petrophysical and geomechanical rock parameters normally considered for evaluating successful shale oil and gas plays include the porosity and brittleness index (e.g. Labani and Rezaee, 2015; Peters et al., 2016). In this study, we have estimated continuous values for these properties for the KCF using wireline log data (density and neutron porosity) and the established property equations of Labani and Rezaee (2015), Alshakhs and Rezaee (2019), and Jin et al. (2014).

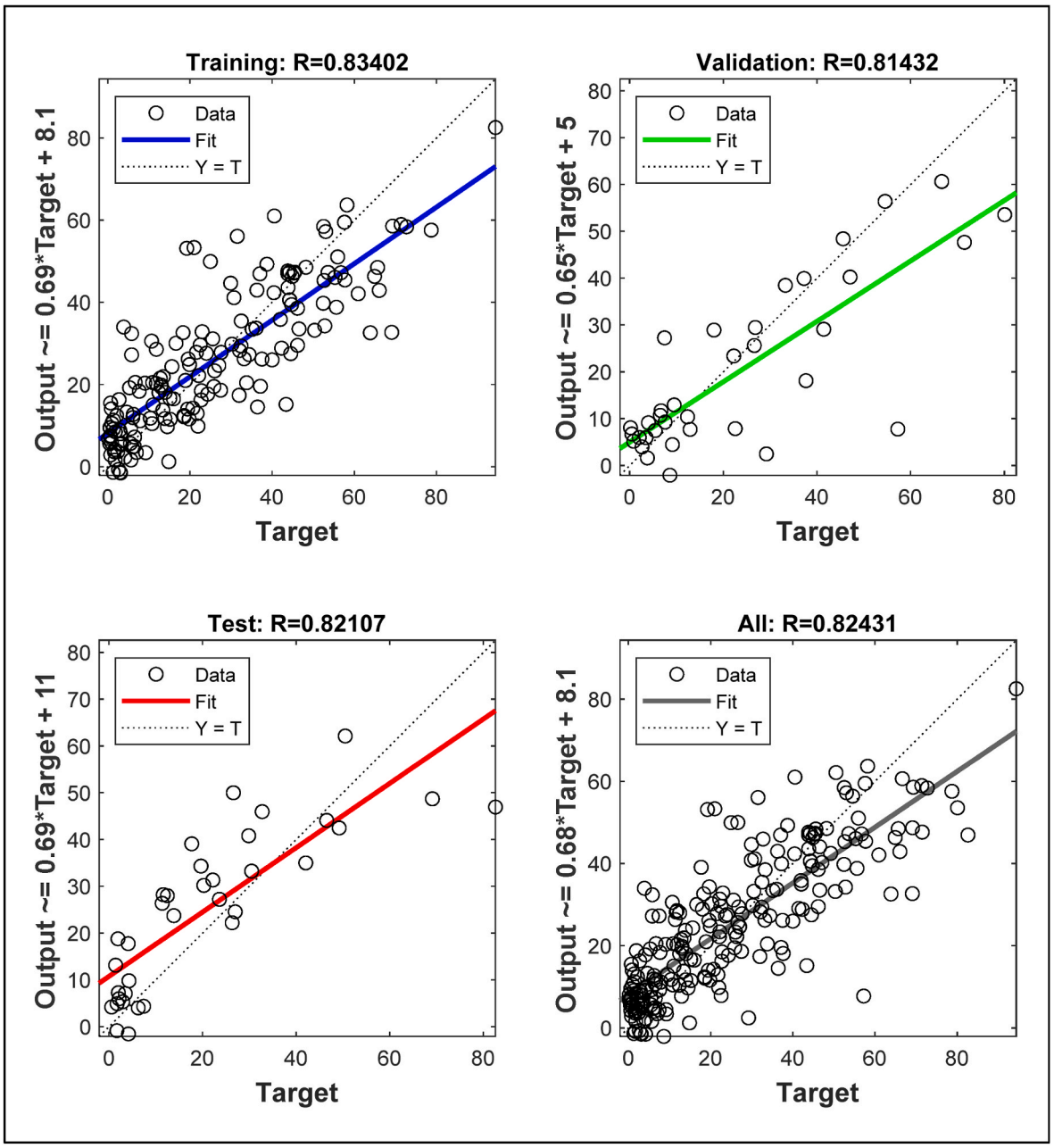

Fig. 8. Regression plots showing the correlation coefficients between target and predicted S_2 values (mg/g) for training, validation and test iterations.

3.1.3.1. Porosity. The total porosity values for the KCF have been estimated from density logs of selected wells using the relationship adapted from Labani and Rezaee (2015).

$$\varnothing_{density=}\frac{(\rho_{ma}-\rho_b)+\rho_b\left(W_{TOC}-\rho_{ma}\frac{W_{TOC}}{\rho_{TOC}}\right)}{\rho_{ma+}\rho_f} \quad (1)$$

where $\varnothing_{density}$ is the total porosity, ρ_{ma} is the solid matrix density, ρ_b is the bulk density log reading, W_{TOC} is TOC weight fraction, ρ_{TOC} is the KCF kerogen density and ρ_f is the fluid density.

TOC input values for Equation (1) have been estimated using the machine learning techniques discussed in Section 3.1.2. Solid matrix, KCF kerogen, and fluid density values are taken from the relevant well reports and published literature (e.g. Andrews, 2014; Labani and Razaee, 2015; Alshakhs and Rezaee, 2019), with values of 2.6, 1.26, and 0.8 g/cm^{3}respectively, as determined.

3.1.3.2. Brittleness index. Although various methods can be used to determine BI based on mineralogical, log, and elastic properties of rocks (Mews et al., 2019), the BI has been derived for the KCF interval in this study using the neutron porosity log correlation proposed by Jin et al. (2014) (Equation (2)).

$$BI = (-1.8748 \times NPHI) + 0.9679 \quad (2)$$

where BI is the brittleness index, and NPHI is the neutron porosity log reading.

Equation (2) is a global correlation derived from the combination of Barnett Shale, Eagle Ford Shale and Woodford Shale which is applicable to formations with high clay content, and correlates well with BI values obtained from mineralogical analysis (Mews et al., 2019).

Continuous total porosity and brittleness index values have been estimated for the KCF in 16 well locations (Figs. 3–4), as for the geochemical property logs.

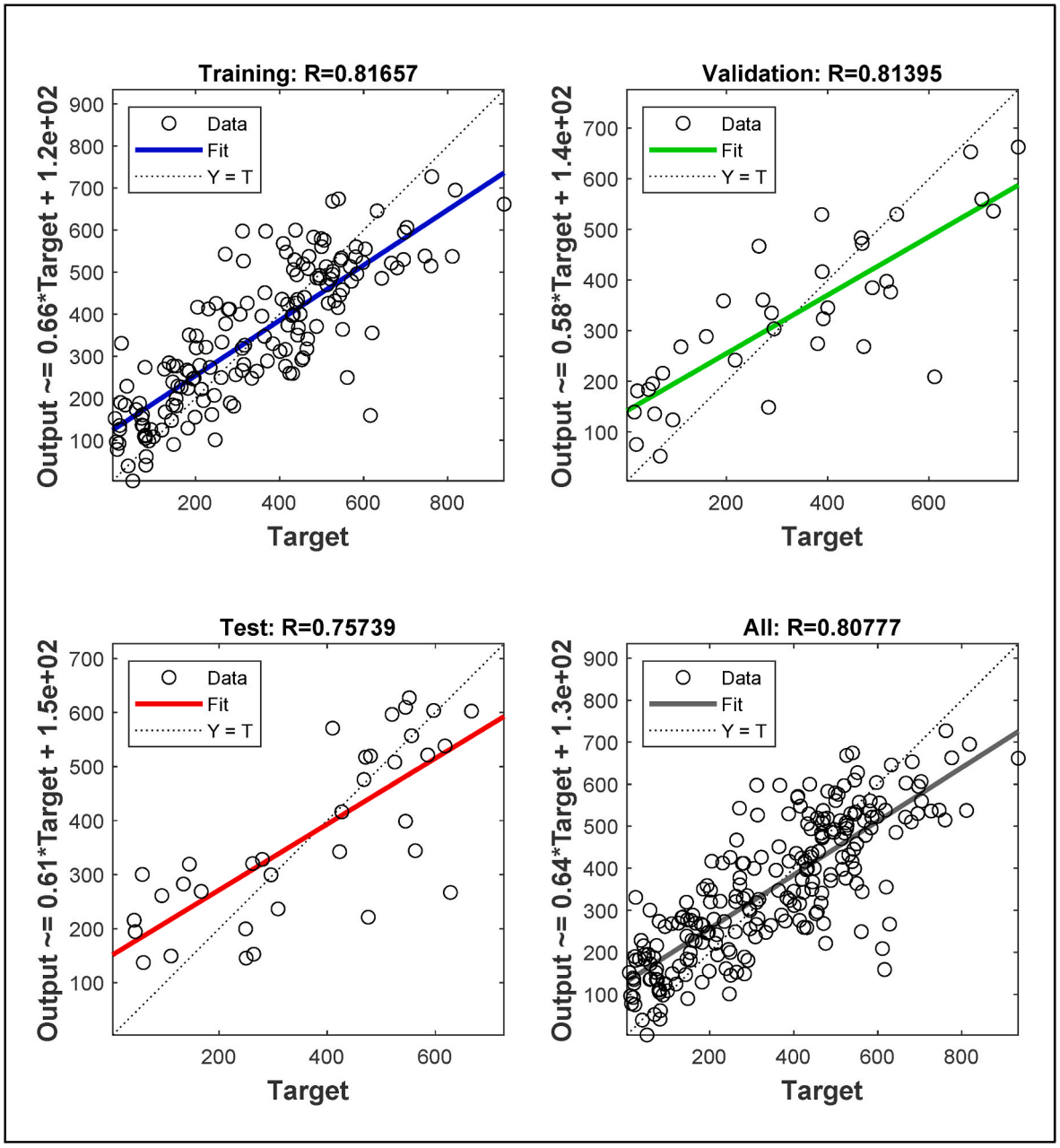

Fig. 9. Regression plots showing the correlation coefficients between target and predicted HI values (mg/gTOC) for training, validation and test iterations.

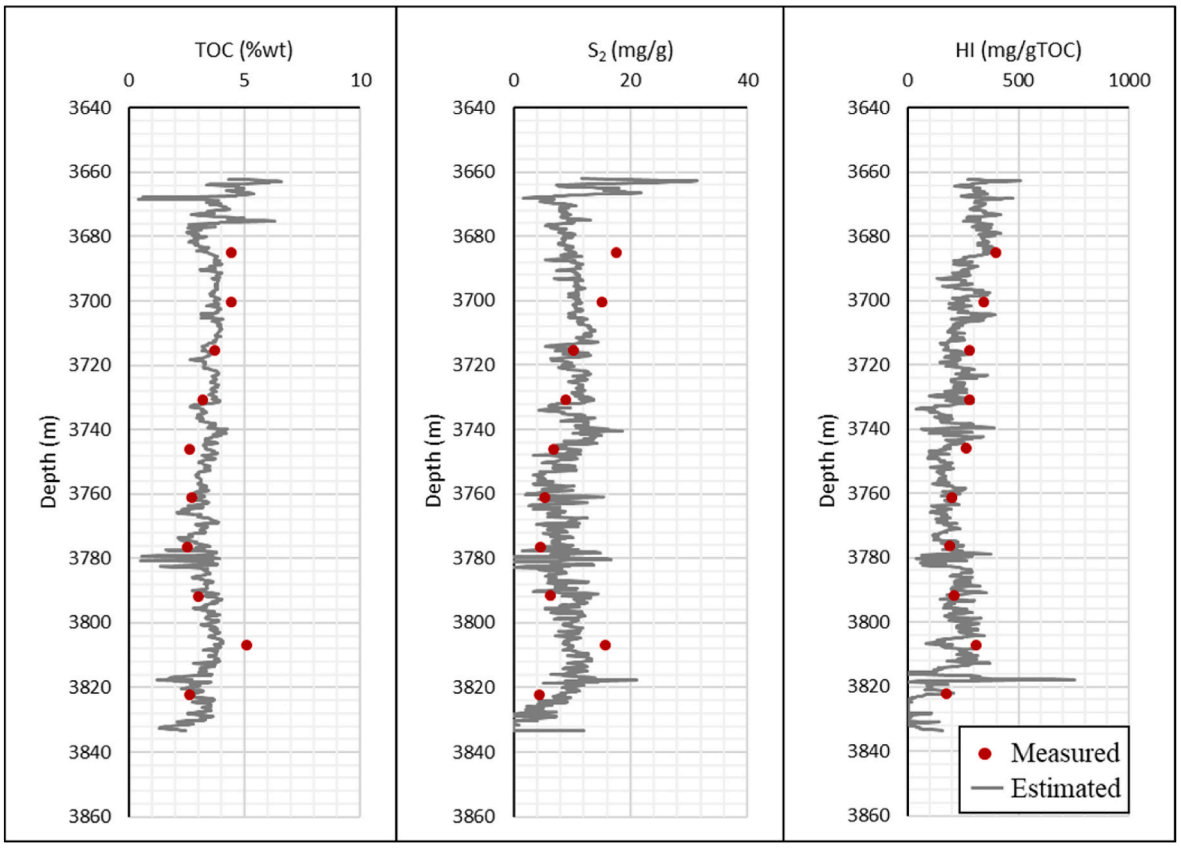

Fig. 10. Comparison between measured geochemical data (TOC, S_2 & HI) from drill cuttings and logs of estimated data using trained neural network models for well 15/18a-6 in the study area. This well was not included in the initial model training.

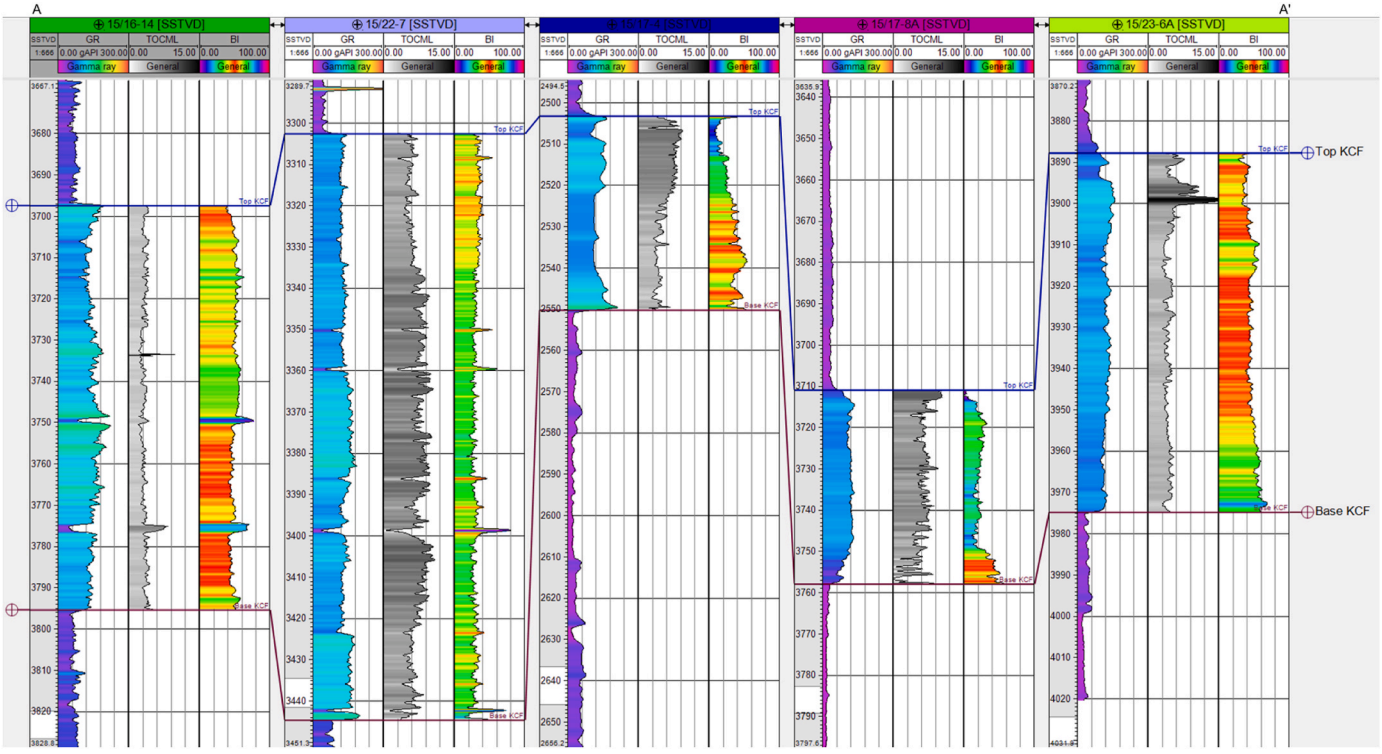

Fig. 11. KCF correlation across the study area (location shown on Fig. 1) showing top, base, and thickness variations, alongside estimated TOC_o and BI reservoir properties.

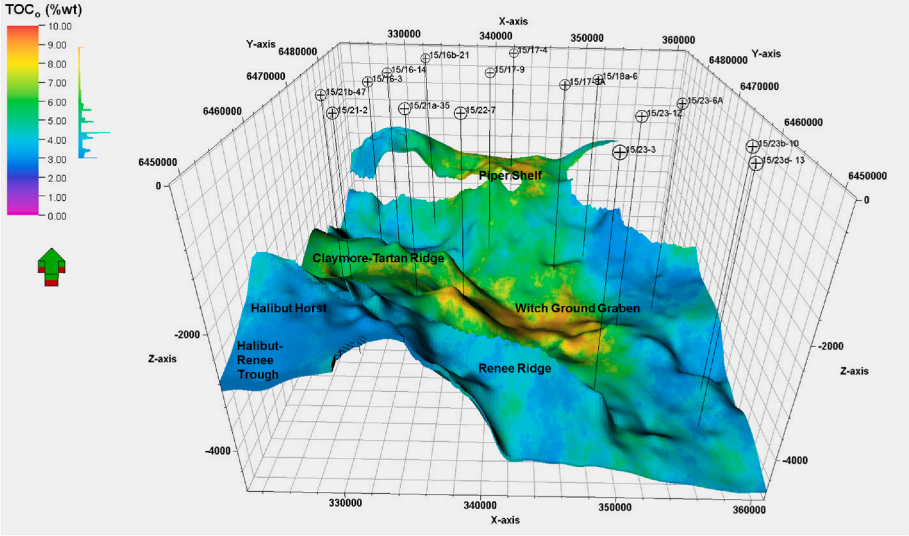

Fig. 12. 3D model showing original TOC distribution for the KCF across the study area.

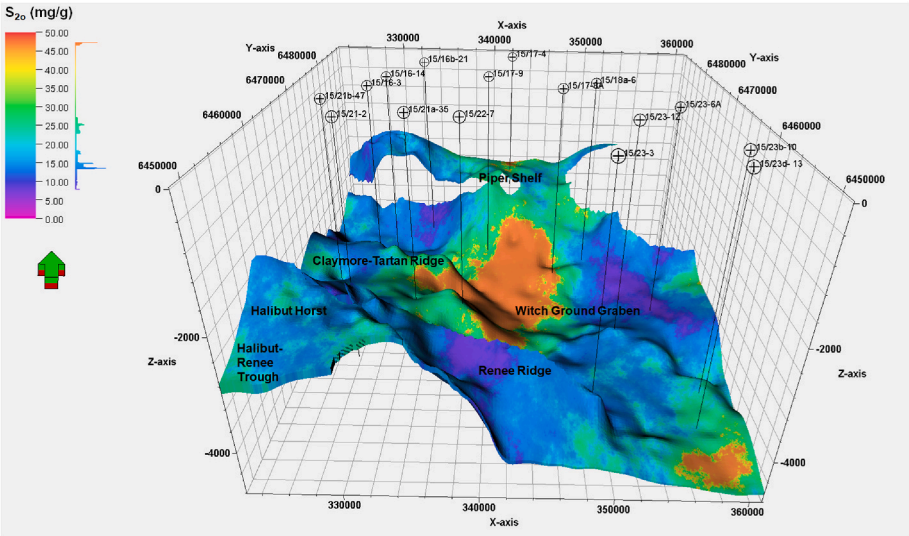

Fig. 13. 3D model showing original S_2 distribution for the KCF across the study area.

3.2. Modelling processes

3.2.1. KCF correlation

The top and base KCF have been correlated across the study area using available well top information compiled from the open file database of the UK Oil & Gas Authority (OGA) and the gamma ray logs (Fig. 11). In addition to the gamma ray logs, the estimated geochemical, petrophysical and geomechanical logs for the KCF have also been correlated across the study area (Fig. 11).

3.2.2. Structural modelling

Due to the limited quality of available seismic data, the structural framework for the 3D geostatistical property model has been defined using the simple gridding technique, which does not require fault interpretations (Schlumberger, 2019). The boundary, top and base limits of the 3D grid for modelling are defined by the input KCF maps (Figs. 3–4).

3.2.3. Petrophysical modelling

This step involves the interpolation of estimated property logs (TOC_o, S_{2o}, HI_o, TP & BI) throughout the 3D model grid. These property logs have been upscaled, and the model for each property has been simulated using the Sequential Gaussian Simulation (SGS) algorithm in Petrel. It is the most used method of simulation in petrophysical modelling, which normally honours more aspects of the input data, particularly the variability of the input data and maintains trends (Fegh et al., 2013; Schlumberger, 2019). More detail description of the procedures involved in petrophysical modelling can be found in Ringrose and Bentley (2015).

4. Results and discussion

4.1. Geochemical properties

4.1.1. Original total organic carbon

Property modelling predicts TOC_o values varying between 3 wt% to 9 wt% for the KCF (Fig. 12), indicating a very good original organic richness for the KCF across the study area. The highest levels of organic richness are found in the central part of the Witch Ground Graben, where the KCF has undergone up to 4.6 km of burial and has a thickness of up to 600 m. High levels of organic richness are also predicted for smaller regions of the Piper Shelf, although here the KCF is thinner and

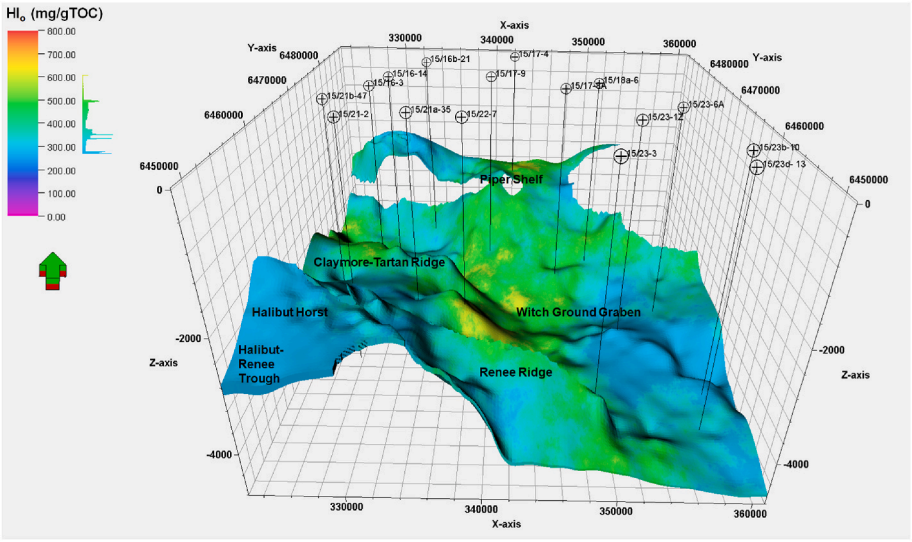

Fig. 14. 3D model showing original HI distribution for the KCF across the study area.

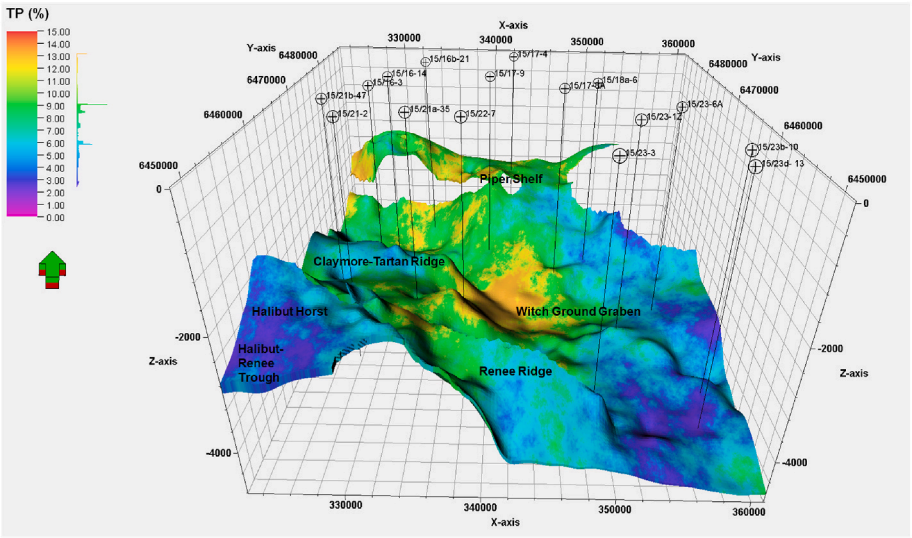

Fig. 15. 3D model showing shale porosity distribution for the KCF across the study area.

buried to less than 3.8 km depth. In these areas, TOC_o values of predominantly greater than 5 wt% are observed (Fig. 12), which is likely attributed to better organic matter preservation. Charpentier and Cook (2011), Andrews (2014), and Jang et al. (2016), suggest that potentially producible shale oil and gas resource plays require TOC_o values greater than 2 wt%.

Our model also predicts up to 5 wt% TOC_o within the Halibut Trough and on the Renee Ridge areas (Fig. 12), although these regions may be subject to higher levels of uncertainty due to reduced well control in these areas. The few wells that are drilled within these areas (Figs. 3–4) lack the complete wireline log data required for estimating the continuous geochemical parameters used in 3D geostatistical property modelling.

4.1.2. Original hydrocarbon yield

In the study area, S_{2o} values ranging between 8 and 48 mg/g have been modelled for the KCF, suggesting very good to excellent original hydrocarbon yield (Fig. 13). The best shale areas are indicated within the central and south-eastern parts of the Witch Ground Graben and localised areas of the Piper Shelf, reflecting the distribution of TOC_o in the study area, with S_{2o} values mostly greater than 20 mg/g (Fig. 13).

4.1.3. Original hydrogen index

The modelled HI_o values for the KCF source rock within the study area range between 270 and 607 mg/gTOC (Fig. 14), suggesting predominantly Type II kerogen content (Peters et al., 2005), and are within the suggested industry threshold for shale plays. Again, the highest values are modelled within the central part of the Witch Ground Graben and Piper Shelf, similar to the trends observed for TOC_o and S_{2o}, (Figs. 12 and 13).

4.2. Petrophysical and geomechanical properties

4.2.1. Total porosity

The 3D model indicates porosity values ranging between 2 and 13% for the KCF within the study area (Fig. 15), with the highest porosity values in the central part of the Witch Ground Graben and Piper Shelf. Overall, the porosity values indicated for the KCF in the study area fall within the range reported for proven shale oil and gas plays, which range from 3% to 15% (e.g. Wang and Gale, 2009; Jarvie, 2012a; Andrews, 2014; Jiang et al., 2016; Alshakhs and Rezaee, 2019).

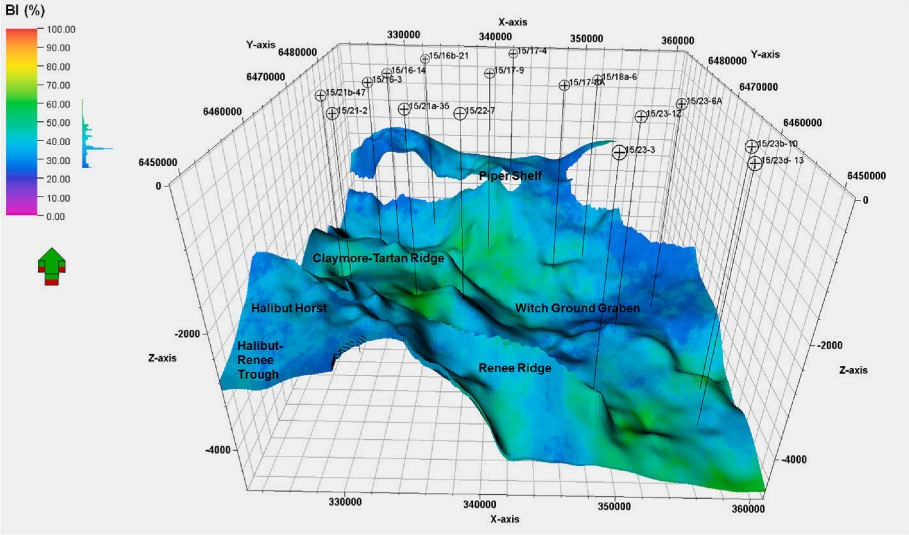

Fig. 16. 3D model showing BI distribution for the KCF across the study area.

4.2.2. *Brittleness index*

The modelling results suggest average BI values for the KCF of between 25 and 62%, with the highest values indicated within the south-eastern and central to northern parts of the Witch Ground Graben (Fig. 16). These values are similar to those reported for the Upper Jurassic to Lower Cretaceous Draupne and Hekkingen Formations in the Norwegian North Sea and Barents Sea (Johnson et al., 2022). Normally, shales with BI values of between 32 and 48% are considered to have moderate frackability, while BI values greater than 48% would indicate high frackability (Perez and Marfurt, 2013). Therefore, modelled BI values suggest favourable conditions for hydraulic fracturing of the KCF across a large section of the study area.

4.3. *Sweet spot identification*

Sweet spots are the best areas with ideal reservoir properties that make it suitable for the optimum extraction of residual oil and gas from unconventional resource plays (Raji, 2018). A sweet spot map has been created to only identify the successful shale areas where the analyzed reservoir properties have prospective overlaps, while the non-prospective areas that do not meet standard industry cut-offs for unconventional resources for all the reservoir properties have been eliminated.

In order to capture shale areas with high levels of original organic richness and hydrocarbon yield potential, cut-off values of 5 wt %, 20 mg/g and 300 mg/g TOC were assigned to TOC_o, S_{2o} and HI_o respectively. The cut-off for TP was set to 3%, while the BI cut value was given to be 32%. The average map generated for each analyzed property, with standard industry cut-offs applied, has been normalized by dividing each map by its maximum estimated value for conversion to a volume fraction map (Fig. 17A–E). An overall sweet spot map is then generated by combining the normalized maps (Fig. 17F).

The sweet spot map shows that the best areas for potentially producible shale oil and gas are located within the central part of the Witch Ground Graben, where the KCF shows greater burial depths of up to 4.6 km and thickness values of up to 600 m, and on parts of the Piper Shelf and Claymore-Tartan Ridge, where the KCF is thinner (<250 m) and shallower with burial depths less than 3.8 km.

It is essential to note that while present-day thermal maturity and residual hydrocarbon saturation have not been modelled for the KCF, the results of previous 1D basin modelling study conducted for four well locations (15/17-8A, 15/17-9, 15/21a-35 and 15/22-7) within the identified sweet spot area have indicated present-day vitrinite reflectance maturity and residual oil saturation values between 0.7 and 1.0 $\%R_o$ and up to 6.4 mg/g respectively, for the KCF (Akinwumiju and Satterfield, 2024), which fall within the range reported for proven shale oil plays.

5. Conclusions

Five key reservoir properties have been analyzed for the KCF in this study in order to identify sweet spot areas after the application of industry standard cut-offs for the modelled parameters in unconventional plays.

Our sweet spot map created by integrating the analyzed KCF reservoir properties using 3D geostatistical modelling, suggests that the best areas for the potential exploitation of shale oil and gas are located within the central part of the ~4.6 km deep Witch Ground Graben, as well as subsidiary regions of the ~3.8 km deep Piper Shelf and Claymore-Tartan Ridge. These areas show the best organic richness and hydrocarbon yield potential with TOC_o, S_{2o} & HI_o values up to 9 wt%, 48 mg/g and 607 mg/gTOC respectively, which is likely attributed to better organic matter preservation. The modelled total porosity values up to 13% and brittleness indices up 65% for the KCF also fall within the range reported for proven shale oil and gas plays in these sweet spots.

Furthermore, the 1D basin models previously constructed for wells 15/17-8A, 15/17-9, 15/21a-35 and 15/22-7 within the identified sweet spot area show that present-day vitrinite reflectance maturity and residual oil saturation values for the KCF vary between 0.7%R_o to 1.0 $\%R_o$ and up to 6.4 mg/g respectively (Akinwumiju and Satterfield, 2024). These values are within the range reported for proven shale oil plays.

The integrated sweet spot map incorporates key parameters for shale oil and gas assessment not previously investigated for the KCF in the UK North Sea. The map simplifies the identification of areas for potential shale oil and gas exploitation from the KCF by interpolation of estimated data from drilled locations, a resource which may prove essential to UK energy security during the net-zero transition.

CRediT authorship contribution statement

Akinniyi A. Akinwumiju: Writing – review & editing, Writing – original draft, Visualization, Validation, Investigation, Formal analysis, Data curation, Conceptualization. **Dorothy Satterfield:** Writing – review & editing, Supervision, Conceptualization. **Jordan J.J. Phethean:** Writing – review & editing.

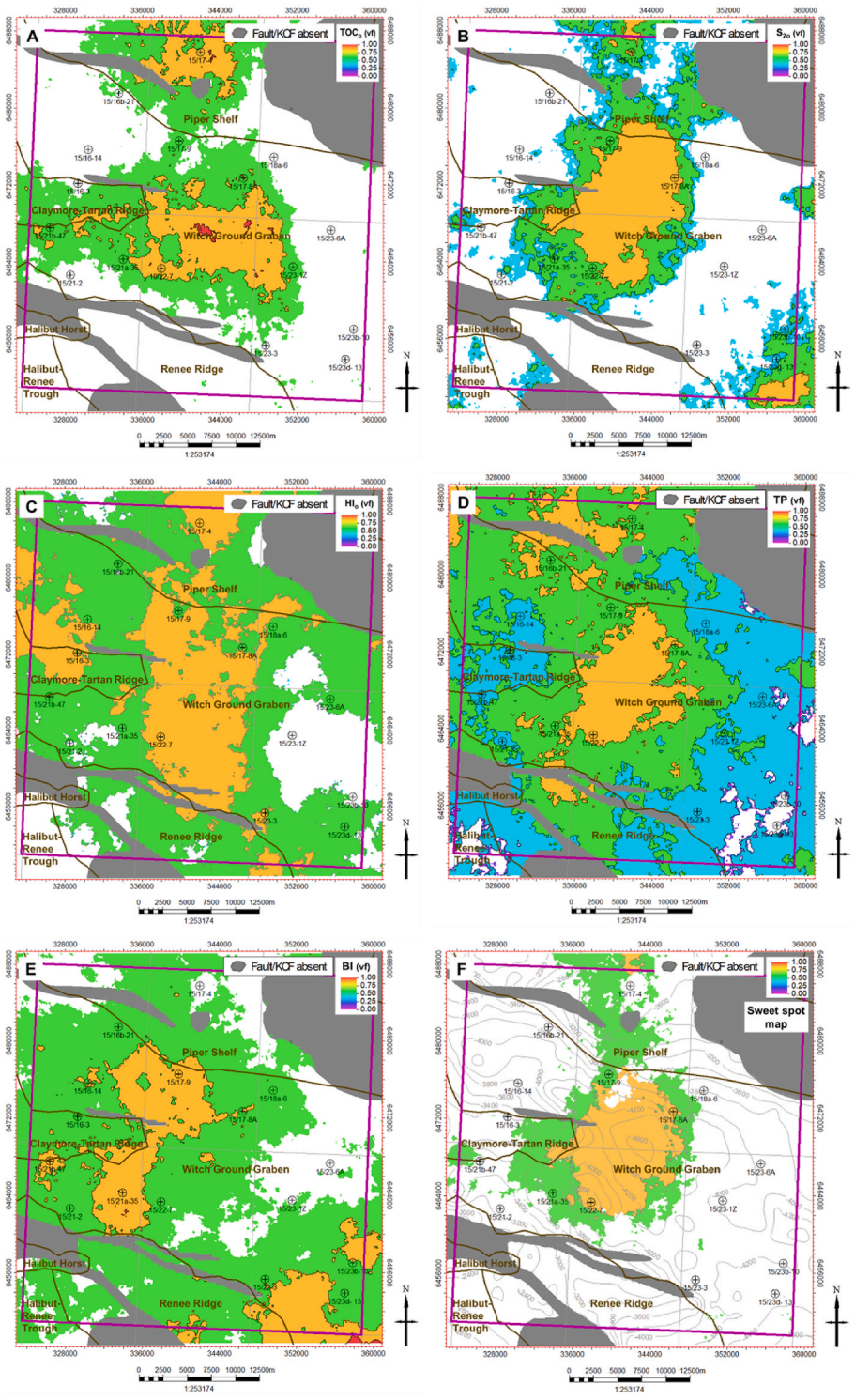

Fig. 17. Normalized average property maps for TOC_o (A), S_{2o} (B), HI_o (C), TP (D) and BI (E), with cut-offs applied. Sweet spot map (F) showing the successful shale areas where all five reservoir properties analyzed for the KCF pass industry thresholds for unconventional resource plays. Grey lines on sweet spot map represent base KCF depth contour in metres.

Declaration of competing interest

The authors declare that they have no known competing financial interests or personal relationships that could have appeared to influence the work reported in this paper.

Data availability

Data will be made available on request.

Acknowledgements

We would like to thank the Oil and Gas Authority, UK for making the database used in this study publicly available. A special thanks goes to

Schlumberger for their generous donation of Petrel license for this study and Integrated Geochemical Interpretation Limited (IGI Ltd) for the use of their p: IGI + software for geochemical data visualization and QC. We also thank ZetaWare and MathWorks for their generous donation of Trinity and MATLAB licenses for this study. The first author acknowledges Lukman Johnson for his constructive feedback on this work. The quality of the manuscript was improved by the suggestions of two anonymous reviewers and Chris Elders.

References

Akinwumiju, A.A., Satterfield, D., 2024. Geochemical Characterization and Paleo-Burial History Modelling of Unconventional Resources: A Case Study from the Kimmeridge Clay Formation (KCF) in the UK North Sea.

Alshakhs, M., Rezaee, R., 2019. Sweet-spot mapping through formation evaluation and property modelling using data from the Goldwyer Formation of the Barbwire Terrace. Canning Basin. Pet. 5, 13–29.

Andrews, I.J., 2014. The Jurassic Shales of the Weald Basin: Geology and Shale Oil and Shale Gas Resource Estimation. British Geological Survey for Department of Energy and Climate Change, London, UK.

Charpentier, R.R., Cook, T.A., 2011. USGS Methodology for Assessing Continuous Petroleum Resources. U.S. Geological Survey Open-File Report, 2011-1167.

Cornford, C., 1998. Source rocks and hydrocarbons of the North Sea. In: Glennie, K.W. (Ed.), Petroleum Geology of the North Sea: Basic Concepts and Recent Advances, fourth ed. Blackwell Science, Oxford, pp. 376–462.

Cornford, C., Birdsong, B., Groves-Gidney, M., 2014. Offshore unconventional oil from the Kimmeridge Clay Formation of the North Sea: a technical and economic case. In: Unconventional Resources Technology Conference Proceedings. August 25-27, 2014.

Erratt, D., Thomas, G.M., Wall, G.R.T., 1999. The evolution of the Central North Sea rift. In: Fleet, A.J., Boldy, S.A.R. (Eds.), Petroleum Geology of Northwest Europe: Proceedings of the 5th Conference. Geological Society, London, pp. 63–82.

Erratt, D., Thomas, G.M., Hartley, N.R., Musum, R., Nicholson, P.H., Spisto, Y., 2010. North Sea hydrocarbon systems: some aspects of our evolving insights into a classic hydrocarbon province. In: Vining, B., Pickering, S.C. (Eds.), Petroleum Geology: from Mature Basins to New Frontiers Proceedings of the 7th Petroleum Geology Conference. Geological Society of London, London, England, pp. 37–56.

Evans, D., Graham, C., Armour, A., Bathurst, P., James, D. (Eds.), 2003. The Millennium Atlas: Petroleum Geology of the Central and Northern North Sea. Geological Society of London, London, Bath, p. 389 (editors and compilers).

Fegh, A., Riahi, M.A., Norouzi, G.H., 2013. Permeability prediction and construction of 3D geological model: application of neural networks and stochastic approaches in an Iranian gas reservoir. Neural Comput. Appl. 23, 1763–1770. https://doi.org/10.1007/s00521-012-1142-8.

Fraser, S.I., Robinson, A.M., Johnson, H.D., Underhill, J.R., Kadolsky, D.G.A., Connell, R., Johannessen, P., Ravnås, R., 2002. Upper Jurassic. In: Evans, D., Graham, C., Armour, A., Bathurst, P. (Eds.), The Millennium Atlas: Petroleum Geology of the Central and Northern North Sea. Geological Society, London, pp. 157–189, 2003.

Gallois, R., 2004. The Kimmeridge Clay: the most intensively studied formation in Britain. Journal Open University Geological Society 25 (2), 33–38.

Glennie, K.W., 1998. Petroleum geology of the North Sea; basic concepts and recent advances. Blackwell Science Geology and Petroleum Geology, Oxford 636–658.

Hu, T., Pang, X.-Q., Jiang, F.-J., Wang, Qi-F., Wu, G.-Y., Liu, X.-H., Jiang, S., Li, C.-R., Xu, T.-W., Chen, Y.-Y., 2021. Key factors controlling shale oil enrichment in saline lacustrine rift basin: implications from two shale oil wells in Dongpu Depression, Bohai Bay Basin. Petrol. Sci. 18, 687–711. https://doi.org/10.1007/s12182-021-00564-z.

Jarvie, D.M., 2012a. Shale resource systems for oil and gas: Part 1—shale-gas resource systems. In: Breyer, J.A. (Ed.), Shale Reservoirs—Giant Resources for the 21st Century, vol. 97. AAPG Memoir, pp. 69–87.

Jarvie, D.M., 2012b. Shale resource systems for oil and gas: Part 2— shale-oil resource systems. In: Breyer, J.A. (Ed.), Shale Reservoirs—Giant Resources for the 21st Century, vol. 97. AAPG Memoir, pp. 89–119.

Jiang, Z., Zhang, W., Liang, C., Wang, Y., Liu, H., Chen, X., 2016. Basic characteristics and evaluation of shale oil reservoirs. Pet. Res. 1, 149–163. https://doi.org/10.1016/S2096-2495(17)30039-X.

Jin, X., Shah, S.N., Roegiers, J.-C., Zhang, B., 2014. Fracability evaluation in shale reservoirs—an integrated petrophysics and geomechanics approach. In: Proceeding of the SPE Hydraulic Fracturing Technology Conference. https://doi.org/10.2118/168589-MS. The Woodlands, Texas, USA, 4–6 February 2014.

Johnson, H., Leslie, A.B., Wilson, C.K., Andrews, I.J., Cooper, R.M., 2005. Middle Jurassic, Upper Jurassic and Lower Cretacous of the UK Central and Northern North Sea. British Geological Survey Research Report, RR/03/001. 42 pp.

Johnson, L.M., Rezaee, R., Kadkhodaie, A., Smith, G., Yu, H., 2018. Geochemical property modelling of a potential shale reservoir in the Canning Basin (Western Australia), using Artificial Neural Networks and geostatistical tools. Comput. Geosci. 120, 73–81.

Johnson, J., Bailey, A., Mondol, N.H., Renard, F., 2022. Using microscopy image analysis to calculate the mineral brittleness index in organic-rich shale. Sixth International Conference on Fault and Top Seals, Vienna, Austria. https://doi.org/10.3997/2214-4609.202243018, 26-28 September 2022.

British Geological Survey, 2022. Kimmeridge Clay Formation [Online]. Available at: https://webapps.bgs.ac.uk/lexicon/lexicon.cfm?pub=KC [Accessed 01 September 2022].

Kadkhodaie-Ilkhchi, A., Rahimpour-Bonab, H., Rezaee, M., 2009. A committee machine with intelligent systems for estimation of total organic carbon content from petrophysical data: an example from Kangan and Dalan reservoirs in South Pars Gas Field, Iran. Comput. Geosci. 35, 459–474.

Khoshnoodkia, M., Mohseni, H., Rahmani, O., Mohammadi, A., 2011. TOC determination of Gadvan formation in South Pars gas field, using artificial intelligent systems and geochemical data. J. Petrol. Sci. Eng. 78 (1), 119–130.

Labani, M., Rezaee, R., 2015. Petrophysical evaluation of gas shale reservoirs. In: Rezaee, R. (Ed.), Fundamentals of Gas Shale Reservoirs. John. Wiley & Sons, Inc., USA, pp. 117–137.

Mackay, L.M., Turner, J., Jones, S.M., White, N.J., 2005. Cenozoic vertical motions in the Moray Firth basin associated with initiation of the Iceland plume. Tectonics 24, TC5004. https://doi.org/10.1029/2004TC001683.

Mahmoud, A.A.A., Elkatatny, S., Mahmoud, M., Abouelresh, M., Abdulraheem, A., Ali, A., 2017. Determination of the total organic carbon (TOC) based on conventional well logs using artificial neural network. Int. J. Coal Geol. 179, 72–80.

MathWorks, 2020. MATLAB Software R2020b.

Mews, K.S., Alhubail, M.M., Barati, R.G., 2019. A review of brittleness index correlations for unconventional tight and ultra-tight reservoirs. Geosci. 9, 319.

Perez, R., Marfurt, K., 2013. Calibration of Brittleness to Elastic Rock Properties via Mineralogy Logs in Unconventional Reservoirs. Search and Discovery. Article #41237.

Peters, K.E., Walters, C.C., Moldowan, J.M., 2005. The Biomarker Guide: Biomarkers and Isotopes in the Environment and Human History. Cambridge University Press, United Kingdom.

Peters, K.E., Xia, X., Pomerantz, A.E., Mullins, O.C., 2016. Geochemistry applied to evaluation of unconventional resources. In: Ma, Y.Z., Holditch, S.A. (Eds.), Unconventional Oil and Gas Resources Handbook. Elsevier Inc., USA, pp. 71–126. https://doi.org/10.1016/B978-0-12-802238-2.00003-1.

Raji, M., 2018. Unconventional Offshore Petroleum-extracting oil from active source rocks of the Kimmeridge Clay Formation of the North Sea, Durham theses, Durham University. Available at Durham E-Theses Online: http://etheses.dur.ac.uk/12476/.

Raji, M., Gröcke, D.R., Greenwell, H.C., Gluyas, J.G., Cornford, C., 2015. The effect of interbedding on shale reservoir properties. J. Mar. Pet. Geol. 67, 154–169.

Ringrose, P.S., Bentley, M., 2015. Reservoir model design: a practitioner's guide. Reservoir Model Design.

Schlumberger, 2019. Property modelling. In: Petrel User Assistance. (Accessed 18 May 2022).

Tu, J.V., 1996. Advantages and disadvantages of using artificial neural networks versus logistic regression for predicting medical outcomes. J. Clin. Epidemiol. 49 (11), 1225–1231. https://doi.org/10.1016/s0895-4356(96)00002-9. PMID: 8892489.

Underhill, J.R., Richardson, N., 2022. Geological controls on petroleum plays and future opportunities in the North Sea rift super basin. AAPG (Am. Assoc. Pet. Geol.) Bull. 106 (3), 573–631. https://doi.org/10.1306/07132120084.

Wang, F.P., Gale, J.F.W., 2009. Screening criteria for shale-gas systems. Gulf Coast Association of Geological Societies Transactions 59, 779–793.

Yu, H., Rezaee, R., Wang, Z., Han, T., Zhang, Y., Arif, M., Johnson, L., 2017. A new method for TOC estimation in tight shale gas reservoirs. Int. J. Coal Geol. 179, 269–277.

Oil & Gas Authority, UK, 2019. UKCS Petroleum Systems Project: Year 1 [online]. Available at: https://data-ogauthority.opendata.arcgis.com/documents/2da8146dc00044cbbfee9e1309602d1c/about. (Accessed 15 July 2019).